International Journal of Engineering and Techniques - Volume 12 Issue 3, May-June - 2026

Application-based Selection of Fin Geometries for Thermal Management: A Focused Review

Dhairya Raval[1], Manish Prajapati[2], Shemal Parmar[3]

([1,2,3] Department of Mechanical Engineering, Polytechnic, The M. S. University of Baroda, Vadodara, India
Email: drraval96@gmail.aom

Abstract: **Fins remain the dominant means of intensifying convective heat transfer, yet the recent expansion of fin geometries — pin, perforated, porous, biomimetic, topology-optimised and adaptive variants alongside the long-standing louvered, wavy and annular families — has outstripped the development of design-selection guidelines. This review consolidates evidence from the recent literature through an application-centred lens. We catalogue the dominant fin types reported for electronics cooling, solar PV and thermal collectors, HVAC and refrigeration heat exchangers, automotive radiators, latent-heat thermal energy storage and gas-turbine blade cooling, together with their performance gains, pressure-drop penalties and operating envelopes. Geometric parameter trends (height, spacing, thickness, aspect ratio) are extracted and the trade-offs that emerge under different binding constraints are made explicit. The synthesis shows that fin selection is best treated as a constraint-satisfaction problem: the dominant fin family in each application is the one that best satisfies the binding constraint (heat flux, pumping power, footprint, manufacturing economics, environmental robustness), not the one with the highest thermal performance in isolation. A six-step practical framework, supported by a literature review table and a look-up table, is presented for engineering use.**

Keywords: **fin selection, thermohydraulic performance, pin-fin, louvered fin, perforated fin, latent heat storage, review.**

I. INTRODUCTION

Effective thermal management has become a binding constraint on modern energy-system design. Microelectronic packages routinely dissipate fluxes above 100 W cm^{-2}, with projections beyond 1000 W cm^{-2} for next-generation processors and three-dimensional integrated circuits [8,18]. Concentrated solar receivers operate under sharply non-uniform circumferential heat fluxes [70,63]; latent-heat thermal energy storage units are bottlenecked by the low thermal conductivity of phase-change materials [12,31,32]. Fins — extended surfaces that enlarge heat-transfer area and disrupt thermal boundary layers — remain the most cost-effective response. The fin repertoire has expanded dramatically over the past two decades to include pin-fin arrays of arbitrary cross-section, louvered and wavy fins augmented with vortex generators, perforated and slotted variants, porous and metal-foam fins that decouple thermal enhancement from hydraulic resistance, biomimetic and topology-optimised geometries enabled by additive manufacturing, and adaptive configurations [8,11,17,89]. Reported single-paper performance gains span from a few percent to several thousand percent depending on geometry and operating regime.

This proliferation has, however, outstripped the development of design-selection guidelines. Most studies optimise a single geometry within a single operating envelope; existing reviews are typically organised by geometry or by a single application class, and the resulting design rules rarely transfer across applications. A practising engineer choosing a fin for a new application is left with a fragmented body of comparative data, performance metrics defined inconsistently across application domains, and no explicit rule for mapping operating constraints onto a fin-geometry choice. The present review addresses this gap. We synthesise recent literature with an explicitly application-centred orientation, focusing on (i) the dominant fin geometries used in each application class and the binding constraint that selects them; (ii) the influence of the principal geometric parameters on thermohydraulic performance; (iii) the trade-offs that emerge across applications; and (iv) a practical decision framework supported by a literature review table and a look-up table.

II. FIN GEOMETRIES: BRIEF OVERVIEW

Five fin families dominate the recent literature. Straight fins (rectangular, trapezoidal, triangular, parabolic) develop a continuously thickening boundary layer along the fin and provide the lowest pressure-drop penalty at the cost of 20–40 % lower air-side heat-transfer coefficient relative to enhanced surfaces; they remain the natural choice as longitudinal fins in shell-and-tube latent-heat storage [15,31,32] and in plain plate-fin compact heat exchangers [3]. Pin fins are short protrusions of cylindrical, elliptical, NACA, droplet, beetle, oblong, I- or twisted cross-section [2,33,39,41,43], generating horseshoe vortices, vortex shedding and inter-pin wake interactions; reported Nusselt-number gains for optimised pin fins range from 44 % [43] to 187 % [55] and 328 % [30], with HTPF regularly above two.

Wavy fins generate Dean-type secondary vortices in their curved sections [71]; they are the air-side default when fouling or condensation is anticipated [84]. Perforated fins use jet-like secondary flow through holes to re-energise the boundary layer while saving 28–60 % of fin mass [5,54]; converging–diverging perforations on annular fins yield a 340 % heat-transfer enhancement [54]. Louvered fins re-initiate the air-side boundary layer at every louver and dominate compact air-side heat exchangers because of the unmatched combination of thermal performance and

continuous-strip-rolled manufacturability [4,50,65]. Porous and metal-foam fins decouple heat-transfer enhancement from pressure-drop penalty by routing flow through a high-permeability skeleton; an anisotropic-gradient porous fin achieves a 76.84 % reduction in thermal resistance and a 3594 % performance gain at Re = 500 over the solid-fin baseline [8].

III. APPLICATION-BASED REVIEW

This section presents the dominant fin selection patterns observed across six application classes, together with the binding constraint that explains the choice. The application-specific performance evidence is summarised in Table I.

A. Electronics Cooling

In electronics cooling the binding constraints are well defined: footprint < 10 cm², heat flux 10–1200 W cm⁻², pumping power capped at a small fraction of dissipated power, and manufacturability at sub-millimetre scale [18]. The pin fin is a consequence of these constraints — it uniquely combines high area density with the boundary-layer-renewal mechanism needed when flow length is too short for fully developed flow. Reported Nu enhancements of 44 % [43], 187 % [55] and 328 % [30] are achieved within realistic pumping budgets. Recent work focuses less on raw Nu and more on positioning along the heat-transfer/pressure-drop Pareto front. Perforation and porous-infill modifications recover Δp without sacrificing h: a stepwise-decreasing-permeability anisotropic-gradient porous fin reduces R_th by 76.84 % and raises performance by 3594 % [8]; porous sidewall ribs raise Nu by 2.7× while cutting f by 55 % [22]. Topology-optimised pin geometries cut R_th by 44 % with negligible Δp [17] or pumping power by 89–97 % at constant heat duty [89], at the cost of additive manufacturing. Under transient or two-phase conditions, the figure of merit reorganises: PCM-pin-fin sinks reduce peak T by 33.8 °C in the first thermal shock but degrade 28 % by the second shock and 33 % by the third [82]; jet–pin-fin microchannels reach CHF = 1098 W cm⁻² at Δp = 4.2 kPa [30,51].

B. Solar PV and Thermal Collectors

Solar applications resist a single dominant fin family because the binding constraint changes within the application class. Where the constraint is air-side h on a planar absorber, boundary-layer-renewal geometries dominate: louvered fins on solar-air-heater absorbers raise η by 106.7 % over plane absorbers [87]; V-angled perforated fins on double-pass collectors deliver 4.45–9.83 % daily-η improvements [26]; hybrid pin-fin–wavy absorber plates achieve Nu = 196.31 at Re = 16 000 [27]. Where the constraint is non-uniform circumferential flux on parabolic-trough absorbers, porous metal-foam fins dominate: semi-annular fin-shape metal foam delivers Nu enhancements of 256–839 % [70], and triangular porous-fin geometries give the highest outlet T with negligible Δp [63]. Where the constraint is temperature uniformity across a high-flux PV array, the choice shifts to low-porosity (ε ≈ 0.6) metal foam or pin fins selected for spreading rather than transport [79]. Across this category, however, a reporting issue dominates: solar-air-heater and DPSAC studies almost universally report η_thermal without quantifying fan-power penalty, leaving effective efficiency unverifiable. The parabolic-trough literature is more honest in reporting friction penalties of 440–789 % alongside Nu gains [70]; the design is viable only because the useful Q dwarfs the pumping cost in concentrated solar service.

C. HVAC and Refrigeration Heat Exchangers

HVAC binding constraints are radically different from electronics: low–moderate Re (100–6500), air-side h is rate-limiting, mass-production economics favour roll-formed aluminium and operating environments may include condensation, frosting or fouling. Within this envelope louvered fins reach asymptotic dominance — they appear in roughly half of the surveyed HVAC studies — because each louver re-initiates the boundary layer and the geometry is only marginally more expensive than plain fins. PIV studies confirm that the duct-directed-vs-louver-directed flow regime is governed by louver angle, fin pitch and Reynolds number [4]; louver-edge geometry separately controls Δp (horizontal edge cuts Δp 24.2 % [56]). Where the louvered fin reaches its limits, the literature switches families. Under frost the pitch optimum collapses: at F_p = 5 mm, Q drops 54.4 % and Δp rises 600 %; at 20 mm the same exchanger loses only 28 % Q with 215 % Δp rise [7] (Fig. 1). Microchannel louver fins clog completely in 240 s under low T_wall and high humidity [61]. Three responses dominate: perforated louvered fin variants (LF-2CH) for drainage [10]; wavy-fin alternatives that retain better thermal-hydraulic balance under wet operation [84]; and surface engineering — a super-amphiphobic louvered fin gives essentially no benefit clean but +16.5 % Q under fouling [85].

D. Automotive Radiators

All five automotive-radiator papers in our corpus use louvered fins on flat tubes [1,50,52,56,65]. The geometry has matured to the point that recent gains come from cross-section refinements such as leaf-shaped (Δp −17.2 %, PEC +3.71 % vs parallelogram [1]), composite straight-and-louvered (+17.5–60.2 % performance vs baseline [65]), or horizontal louver edges (Δp −24.2 % [56]). The order-of-magnitude gains routinely reported for novel pin-fin geometries in electronics are not available here. Further radiator improvements depend instead on coolant-side modification, e.g. the 40 % temperature-drop increase obtained from a 0.1 % MWCNT-SiO_2 hybrid nanofluid [50], or system-level integration as in the wavy-louvered + VG combination for PEMFC radiators [52].

E. Latent-heat Thermal Energy Storage

Annular fins dominate LHTES because they extend conduction radially into a low-conductivity PCM. Variable-diameter Cu fins cut charging time by 89.45 % [35]; branched annular fins cut melting time 27.13 % [80]; petal-shaped fins

cut solidification time 22.8 % vs longitudinal [72]; snowflake-annular fins cut melting and solidification times 47.52 % and 27.94 % respectively [66]. The defining trade-off is that solid annular fins suppress the buoyancy-driven flow that would otherwise extend heat into the upper PCM region — this becomes binding above a fin volume fraction of approximately 4–5 % (Fig. 4). The recent literature accordingly favours perforated, branched, hollow or biomimetic-topology variants that reopen flow paths [11,21,31,46]: biomimetic vertically-aligned annular fins shorten melting time by 45.9 % [11]; perforated annular fins reduce charging time by 5.49 % over solid fins of equal volume [21]; and branched-annular fins improve the uniformity of melt rate by 34.72 % [80]. For transient PCM-pin-fin sinks intended for electronics buffering, the cycle-fatigue trade-off must be checked: 28 %/33 % performance loss after 2nd/3rd thermal shock has been reported [82].

F. Gas-turbine Blade Cooling and Other Applications

Gas-turbine blade trailing-edge cooling uses pin fins exclusively because the geometry simultaneously enhances heat transfer and acts as a structural tie between the suction and pressure surfaces of a thin trailing edge [2,19,23,33,36,39]. Reported gains: curved pins +15.77 % over vertical at Re = 10^4 [23]; beetle pins +6.66 % Q over circular but Δp −76.25 % giving thermal-efficiency-factor +29.4 % [33]; droplet pins less affected by rotation than circular [39]; heterogeneous pin arrays optimised by Bayesian + transfer learning give +6.8 % HT at −76.7 % Δp [42]. Thermoelectric ducts use annular fins with longitudinal vortex-generators or porous inserts to combine flow disturbance with energy harvesting [67,74,78]; the corresponding constraint is that Bi_2Te_3 TE modules are unstable above ≈ 600 K. Active enhancement (corona discharge, piezoelectric fans, ultrasonic vibration) [13,44,81] provides the largest single-paper gains but introduces moving parts and noise; coatings (super-amphiphobic, high-emissivity) [62,85] pay back only when their target degradation regime dominates the duty cycle.

TABLE I

CONSOLIDATED LITERATURE REVIEW OF REPRESENTATIVE STUDIES ON FIN GEOMETRIES

Application	Fin geometry	Operating range	Headline result	Source
Electronics cooling / microchannel heat sinks				
Microchannel	Anisotropic gradient porous plate-fin	Re 100–1000	R_th −76.84 %, performance +3594 %	[8]
Pin-fin sink	Sterling-gun-barrel perforated pin	Re 9 973–19 945	Nu 792.08 (+44 %); HTPF > 1	[43]
Plate-pin-fin	NACA 00XX pin fin	Re 300–3300	THPF_max 1.93	[9]
Microchannel	Non-regular pin (NSGA-II + TOPSIS)	50 candidates	R_t 0.707 K/W; −62.9 % P_p	[51]
Microchannel	Topology-optimised micro-pin	V_f 17.5 %	Pumping power −89 % / −97.6 %	[89]
Pin-fin sink	Adjoint-optimised pin	Re 1000, 5000	R_th −44 %; Δp −36.2 %	[17]
Boiling sink	Embedded jet–pin-fin	ΔT_sub 20–60 °C	CHF 1098 W cm⁻² at Δp 4.2 kPa	[30]
PCM-pin-fin	Cu pins in paraffin PCM	9–36 pins	Peak T −33.8 °C; cycle fade 28/33 %	[82]
Solar PV / thermal collectors				
SAH	Louvered fin on absorber	ṁ 0.007–0.0158 kg/s	η_max 70 %; +106.7 %	[87]
DPSAC	V-angled perforated fins	3 flow rates	Daily η +4.45–9.83 %	[26]
SAH hybrid	Pin-fin + wavy absorber	Re 16 000	Nu_max 196.31; THAF 1.69	[27]
PTC	Semi-annular metal-foam fin	Turbulent	Nu +256–839 %; f +440–789 %	[70]
PTC	Internal porous fins	RNG k-ε	Triangular best; negligible Δp	[63]
HCPV	Pin-fin and metal foam	ṁ 50–250 g/min	ε = 0.6 best uniformity	[79]
PV/T	Louvered + serpentine tube	Outdoor	η_th 89.1 %; cell T −31.7 %	[88]
HVAC and refrigeration				
Fin-tube HX	Plain / louver / VG	F_p 1.6–2.0 mm	Louver h +2–15 % vs VG	[6]
Fin-tube (frost)	Perforated plate fin	F_p 5 vs 20 mm	Q +38.9 %; collapse at F_p 5	[7]
LFFTHX	Perforated louvered LF-2CH	Louver 18°, 24°	Q +20.9 % / +18.0 %	[10]
MCHX (frost)	Microchannel louvered	T_w −8/−12 °C	Clog 240→160 s	[61]
Wavy HX	Wavy fin + concave VG	Re sweep	Nu +30.4 %, JF +25.9 %	[71]
Wet HX	20 wavy-fin geometries	VOF + species	G3, G4 optimal f and j	[84]
Fouled HX	Super-amphiphobic louvered	RH 30–80 %	Q +16.5 % (fouled)	[85]
Hybrid HX	Curved-VG louvered	Re 1800–6450	Nu +61–92 % vs plain	[86]
Automotive radiators				
Car radiator	Leaf-shaped louvered	Angle 15.9°	Δp −17.2 %, PEC +3.71 %	[1]

Application	Fin geometry	Operating range	Headline result	Source
Car radiator	Louvered + MWCNT-SiO_2	5–20 L/min	ΔT +40 %	[50]
PEMFC radiator	Wavy-louvered + L-VG	CFD	L-VG highest h	[52]
Flat-tube	Composite straight + louvered	1–6 m/s	+17.5–60.2 % vs baseline	[65]
Latent-heat thermal energy storage (LHTES)				
Shell-tube	Branch-annular fin	Branch h, location	Melt time −8.67–35.39 %	[12]
LHTES	Biomimetic topology-optimised	Optimisation	Melt time −45.9 %	[11]
LHTES	Petal-shaped fin	Volume ratio	First 30 % solid −43.3 %	[72]
LHTES	Perforated spiral fin	Inclination 0–180°	η 63.4 %; Nu_avg +44 %	[34]
LHTES	9 concentric annular fins	Same volume	Times −72.83 % / −86.39 %	[20]
LHTES	Variable-D Cu fins	Same Cu volume	Charge −89.45 %	[35]
Triplex tube	Longitudinal fin	Re 500–2000	Solidification −55.3 %	[15]
LHTES	Annular-snowflake fin	Charge + discharge	Times −47.52 % / −27.94 %	[66]
Gas-turbine and other applications				
Turbine blade	Pin fins (vert/curv/incl)	Re 10^4–5×10^4	Curved +15.77 % at Re 10^4	[23]
Turbine blade	Beetle / teardrop / oblong	Re 10^4–8×10^4	Beetle +29.4 % factor	[33]
Turbine blade	Heterogeneous pin	Surrogate	HT +6.8 %; Δp −76.7 %	[42]
Annular TEG	LVG-like fin / Bi_2Te_3	ΔT 330 K	P_net 4.54 W; η 3.18 %	[67]
NC sink	Perforated rectangular	φ 4–12 mm	12 mm @ 45°: h +32 %	[5]

IV. INFLUENCE OF GEOMETRIC PARAMETERS

This section condenses the parameter trends drawn from the corpus into the four most consequential geometric variables. The principal trade-offs are visualised in Figs. 1–4.

Fin pitch produces the sharpest spacing-vs-pressure-drop trade-off in the dataset, particularly under fouling or frosting. A perforated fin-tube heat exchanger at F_p = 5 mm under frost loses 54.4 % of its heat-transfer rate while pressure drop rises 600 %; at F_p = 20 mm the same exchanger loses only 28 % with a 215 % Δp rise [7]. Fig. 1 visualises this bifurcation: the clean-state heat-transfer coefficient rises monotonically as the pitch is reduced, but the frosted-state curve collapses below approximately 10 mm pitch as the ice front bridges adjacent fins [7,10,61,85]. In pin-fin condensation the optimum spacing is 2 mm: smaller spacings impair drainage [15,29]. In ice storage, 4 mm spacing delivers 26.3 % greater capacity than 12 mm [76].

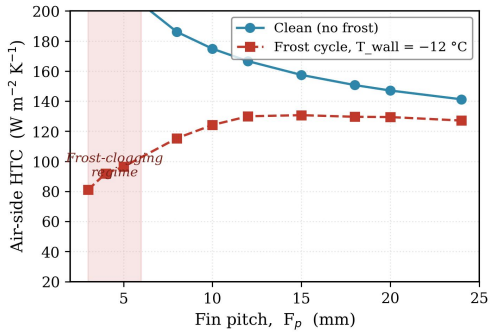

Fig. 1. Air-side heat-transfer coefficient versus fin pitch for clean and frosted operation. The clean curve rises monotonically with reduced pitch, while the frost-cycled curve collapses below approximately 10 mm pitch as the ice front bridges adjacent fins. Compiled from [7,10,61,85].

Fin height shows a non-monotonic optimum across most fin families. Increasing height initially adds surface area linearly, but past the boundary-layer-interaction threshold either the upper fin runs at near-fluid temperature and contributes little, or it physically blocks secondary or buoyancy flow. In a microchannel anisotropic-gradient porous fin, increasing the height ratio from 0.3 to 2.0 produces a 5159 % performance gain [8]; in a finned-tube HX the global-performance-coefficient peaks at ~10 mm height and declines on either side [53]. In LHTES, solid full-height annular fins suppress buoyancy-driven flow and the entire branched-, hollow- and perforated-fin literature is, in effect, a response to this issue [11,21,80].

Fin thickness shows a single optimum: in plate-pin-fin sinks a relative thickness of 0.45 (with streamwise pitch 0.25) gives THPF_max = 1.93 at Re = 1500; above 0.45 performance falls due to flow blockage [9]. Aspect ratio is most clearly tied to flow regime: in an aviation power-converter pin-fin sink, the height-to-diameter ratio rh = 10 is optimum at $Re \le 10^4$ but performance falls monotonically with rh at $Re \ge 1.5\times10^4$ [59]; in tapered pin fins for PVT MCHS, smaller taper angles win at low Re, larger at high Re [64]. The recurring conclusion is that aspect-ratio optima are flow-regime-dependent, not universal — graded and topology-optimised geometries beat uniform geometries by margins (50–200 % pumping-power reduction at iso-Q) larger than any single shape change [8,73,89].

Fig. 2 visualises the cumulative effect of these parameter trade-offs in the (Nu/Nu_0, f/f_0) plane. Each fin family occupies a characteristic region: conventional pin and louvered geometries cluster near the iso-PEC reference line, while porous, anisotropic-gradient and topology-optimised designs sit below it (high Nu/Nu_0 at modest f/f_0), supporting the view that decoupling mechanisms — rather than further

refinements of conventional geometry — are the principal source of recent performance gains.

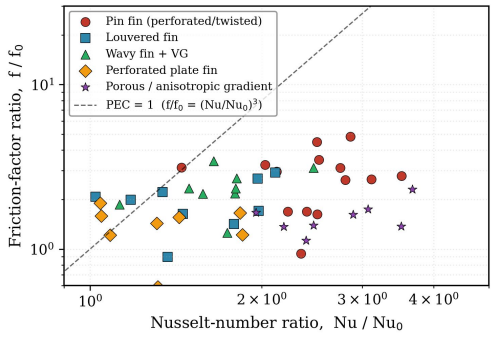

Fig. 2. Friction-factor ratio f/f_0 versus Nusselt-number ratio Nu/Nu_0 for representative members of five fin families. The dashed line corresponds to PEC = 1. Porous and anisotropic-gradient designs cluster below the line, consistent with their reported decoupling of heat-transfer enhancement from pressure-drop penalty [8,22,24,30,41,43,55,71,86].

Fig. 3 generalises the picture across operating regimes: HTPF as a function of Reynolds number shows that pin fins peak in the laminar microchannel range, louvered and wavy + VG fins plateau in the moderate-Re HVAC range, and porous / gradient designs maintain elevated HTPF over a broader Re range. This broader Re band is the principal advantage of the porous family beyond raw Nu enhancement.

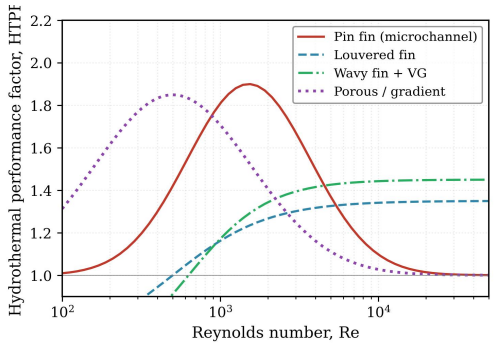

Fig. 3. Hydrothermal performance factor (HTPF) as a function of Reynolds number for representative members of four fin families. Pin fins peak in the laminar microchannel range, louvered fins plateau in the moderate-Re HVAC range, and porous/gradient designs maintain elevated HTPF over a broader Re range [8,40,41,51,71].

In LHTES specifically, the cumulative effect of geometric parameters appears as a monotonic decrease in melting time with fin volume fraction up to a buoyancy-blockage threshold (Fig. 4). Plain annular fins exhibit diminishing returns and a clear plateau above approximately 4–5 % fin volume; branched, perforated and biomimetic-topology variants continue to deliver gains by reopening flow paths [11,12,21,31,80].

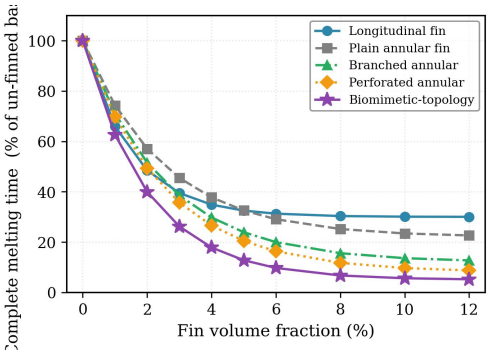

Fig. 4. Complete melting time (% of un-finned baseline) versus fin volume fraction for five LHTES fin topologies. Plain annular fins show diminishing returns above ~4 % volume due to buoyancy blockage; branched, perforated and biomimetic-topology variants continue to deliver gains [11,20,21,31,80].

V. DECISION FRAMEWORK FOR FIN SELECTION

The framework distils the application-specific evidence of Section III and the parameter trends of Section IV into a six-step procedure. The accompanying look-up table (Table II) consolidates the application-specific recommendations together with the failure modes most likely to invalidate them.

1) Identify the application class: Place the device in one of the application classes catalogued in Section III: chip-level / microchannel electronics; general electronic / motor heat sink; solar absorber-plate or air-heater; parabolic-trough or HCPV solar receiver; HVAC fin-tube heat exchanger; automotive or fuel-cell radiator; latent-heat thermal energy storage; gas-turbine blade trailing-edge cooling; or thermoelectric / waste-heat duct.

2) Quantify the binding constraint: Record four numbers: heat flux per unit footprint (W cm^{-2}); fluid-side Reynolds-number range; pumping-power or fan-power budget; and operating-environment severity (clean, fouled, frost, condensation, cyclic). Decide which is the single binding constraint. Where two are binding simultaneously, treat the problem as multi-objective.

3) Map the flow condition to a fin family: Under natural convection only, choose rectangular or annular fins with perforations [5]. Under forced laminar flow ($Re < 2000$), pin fins are the default; porous or semi-porous fins should be considered when pressure drop is the binding constraint [8,22]. Under forced turbulent flow ($Re > 2000$), louvered fins are preferred for compact air-side service; wavy fins with VG for higher Re; perforated pin fins for high-flux electronics [71,40]. Under two-phase boiling, micro pin-fin arrays with porous coatings or jet–pin-fin manifold combinations give the highest CHF [30]. Under PCM melting/solidification, annular fins with perforations or branches preserve buoyancy flow [11,12,21]; pin fins are acceptable for transient buffering only when cyclic degradation is tolerable [82]. Under condensing or frosting flow, wavy fins or perforated louvered (LF-2CH) fins are recommended; specify pitch ≥ 20 mm if frost cycles are expected (Fig. 1) [7,10,61,84,85].

*4) **Apply the space constraint:*** At sub-millimetre scale, use pin fins via Si etching, polymer micro-moulding or selective laser melting; topology-optimised geometries when additive manufacturing is feasible [17,89]. At mm–cm scale, continuous-strip rolled aluminium louvered fins on flat tubes are the default for HVAC and automotive radiators [50,65]. At dm–m scale, annular or longitudinal fins welded or extruded onto tubes, with perforated variants where buoyancy must be preserved (Fig. 4) [11,21]. Mass-critical applications: perforated fins of any base geometry, saving 28–60 % mass at small h cost [5,54].

*5) **Apply the cost / manufacturing constraint:*** Lowest cost, mass production: louvered fins on aluminium strip [50,65]. Moderate cost: extruded pin fins, cast plate-pin combinations, perforated stamped fins. High cost, low-volume, performance-driven: topology-optimised, biomimetic or anisotropic-gradient porous fins [8,11,89]. Coatings (hydrophobic, amphiphobic, high-emissivity) pay back only under specific operating regimes — evaluate against time-averaged duty rather than nameplate [62,85].

*6) **Validate against application-specific failure modes:*** Electronics under cyclic load: confirm tolerance to repeated thermal shocks (PCM-pin-fin sinks degrade 28 %/33 % by 2nd/3rd shock [82]). HVAC: below 5 mm pitch, performance falls by half under frost (Fig. 1) [7]. Automotive: if geometric tweaks alone cannot meet the target, reconsider coolant chemistry [50]. PCM storage: solid annular fins block buoyancy; if charging cycle exceeds 24 h, replace with branched, perforated or hollow variants [11,21]. Solar receivers: confirm η_eff (thermal − pumping) is reported and positive [70]. Gas-turbine blades: respect the 1100 °C nickel-alloy limit; the geometry must double as a structural tie [2]. Thermoelectric ducts: Bi_2Te_3 unstable above ≈ 600 K [67].

TABLE II

APPLICATION-SPECIFIC LOOK-UP OF FIN-FAMILY RECOMMENDATIONS

Application class	Flow regime	Space / cost tier	Recommended fin family	Key caveat
Chip / microchannel electronics	Forced laminar; 2-phase	Sub-mm; high cost	Pin fin (perforated, porous, topology-opt.)	PCM-pin-fin: 28–33 % cycle fade
General electronic / motor sink	Forced air, turbulent	cm-scale; moderate	Perforated rectangular or pin; louvered for volume	Solid pins raise Δp at high Re
Solar air heater / DPSAC	Forced air, turbulent	Plate; low cost	V-angled / louvered perforated	Report η including fan power
Parabolic-trough collector	Forced liquid, turbulent	Tube; medium cost	Porous metal-foam fin	f-penalty 440–789 %
PV/T or HCPV cooling	Forced liquid, low–mod flow	Panel; low–med cost	Louvered (PV/T) or low-porosity foam (HCPV)	Optimise for T uniformity
HVAC fin-tube HX (clean)	Forced air, low–mod Re	Compact; lowest cost	Louvered fin on flat tube	Verify louver-directed flow
HVAC HX (frost / condensing)	Forced air with moisture	Compact; low cost	Wavy or perforated louvered; pitch ≥ 20 mm	Below 5 mm pitch, Q drops 54 %
Automotive radiator	Forced air + liquid	Compact; lowest cost	Louvered fin (leaf, composite, RSM)	Geometry near saturation
Latent-heat TES	Conduction-dominated melt/solid	Tube–shell; medium	Annular with perforations / branches / hollow	Solid annular blocks buoyancy
Gas-turbine cooling	Forced air; high-T	mm–cm; high cost	Pin fins of nickel alloy	1100 °C limit; structural tie
Thermoelectric duct	Forced hot gas; large ΔT	Annular pipe; medium	Annular + LVG fins / porous inserts	Bi_2Te_3 unstable above 600 K
Natural-convection sink	Natural convection	cm–dm; low cost	Perforated rect. / annular (φ 8–12 mm)	Optimum hole orientation-dependent

VI. CONCLUSIONS

This focused review of recent literature on fin geometries supports four conclusions.

(i) Fin selection is most accurately treated as a constraint-satisfaction problem rather than a single-objective optimisation. The dominant fin family in each application is the one that best satisfies the binding constraint (heat flux, pumping power, footprint, manufacturing economics, environmental robustness), not the one with the highest thermal performance in isolation.

(ii) The four principal geometric parameters — fin height, spacing, thickness and aspect ratio — modulate performance non-monotonically and in application-specific ways (Figs. 1–4). Optima depend on Reynolds number, on the ratio of conduction to convection resistance and on the operating environment. Variable, graded and topology-optimised geometries consistently outperform uniform geometries.

(iii) The largest residual gains are likely to come from designs that decouple heat-transfer enhancement from pressure-drop penalty rather than push along the existing Pareto front (Fig. 2). Anisotropic gradient porosity, surface engineering and active enhancement are early instances. The community would benefit from a unified framework for comparing such decoupling mechanisms and from cycle-aware metrics for transient applications.

(iv) The six-step framework of Section V and the look-up of Table II provide an engineering-ready tool for fin selection across applications. Combined with the consolidated literature review of Table I they convert what is currently a heterogeneous and largely incommensurable body of evidence into a coherent decision aid.

ACKNOWLEDGMENT

The author thanks the Department of Polymer Engineering, M. S. University of Baroda, for institutional support during the preparation of this review.

REFERENCES

[1] Wang et al., A study on the comprehensive heat dissipation performance of new louvered fins for automotive radiator, Case Studies in Thermal Engineering (2026). https://doi.org/10.1016/j.csite.2026.107782.

[2] Chatti et al., Advanced turbine blade design: LBM simulation of pin fin sharps' impact on heat transfer and flow in gas turbine, Thermal Advances (2025). https://doi.org/10.1016/j.thradv.2025.100031.

[3] Doan et al., Air side thermal and hydraulic performance assessment of skived, louver, offset honeycomb, and metal foam finned mini-channel heat exchangers, Engineering Science and Technology (2025). https://doi.org/10.1016/j.jestch.2025.102242.

[4] An experimental – computational and flow visualization, International Journal of Heat and Mass Transfer (2018). https://doi.org/10.1016/j.ijheatmasstransfer.2017.12.127.

[5] An experimental investigation of natural convection heat, Experimental Thermal and Fluid Science (2015).

[6] An experimental study of the air side performance of f, International Journal of Heat and Mass Transfer (2015).

[7] Liu et al., An experimental study on the air side heat transfer performance of the perforated fin-tube heat exchangers under the frosting conditions, Applied Thermal Engineering (2020). https://doi.org/10.1016/j.applthermaleng.2019.114634.

[8] Bahrami et al., Anisotropic gradient porous fins for microchannel heat sinks: A new paradigm in thermal management design, International Journal of Heat and Mass Transfer (2026). https://doi.org/10.1016/j.ijthermalsci.2026.110706.

[9] Dixit et al., Assessing thermohydraulic performance in plate heat sinks with NACA pin-fins: A synergistic experimental and predictive modelling approach, International Communications in Heat and Mass Transfer (2025). https://doi.org/10.1016/j.icheatmasstransfer.2025.109817.

[10] Zhou et al., Assessment of the heat transfer efficiency of perforated louvered fins for improved drainage, International Journal of Heat and Mass Transfer (2024). https://doi.org/10.1016/j.ijheatmasstransfer.2024.125654.

[11] Liu et al., Biomimetic optimized vertically aligned annular fins for fast latent heat thermal energy storage, Applied Energy (2023). https://doi.org/10.1016/j.apenergy.2023.121435.

[12] Li et al., Branch design of annular fins for heat storage enhancement of the shell-and-tube latent heat thermal energy storage unit, Journal of Energy Storage (2025). https://doi.org/10.1016/j.est.2025.116904.

[13] Lanbaran et al., Comparative analysis of heat transfer enhancement using direct current and alternating current corona discharge in pin fin arrays, International Journal of Heat and Mass Transfer (2025). https://doi.org/10.1016/j.ijthermalsci.2025.109864.

[14] Attia et al., Comparative evaluation and productivity optimization of conical solar stills using a novel design of tent-shaped wick material combined with circular pin columns as fins and heat storage materials, Separation and Purification Technology (2025). https://doi.org/10.1016/j.seppur.2025.134595.

[15] Said et al., Design optimization and performance analysis of a PCM-to-air heat exchanger with optimized fin configuration for building heating applications, International Communications in Heat and Mass Transfer (2025). https://doi.org/10.1016/j.icheatmasstransfer.2025.109764.

[16] Ao et al., Design optimization of a novel annular fin on a latent heat storage device for building heating, Journal of Energy Storage (2023). https://doi.org/10.1016/j.est.2023.107124.

[17] Nguyen et al., Designing pin fin heat sinks with restarting adjoint optimization approach, International Journal of Heat and Mass Transfer (2025). https://doi.org/10.1016/j.ijheatmasstransfer.2025.126856.

[18] Ao et al., Dual-layer cylindrical array of pin–fin microchannels with heat dissipation capacity up to 1200 W/cm2, International Journal of Heat and Mass Transfer (2025). https://doi.org/10.1016/j.ijheatfluidflow.2025.110003.

[19] Yan et al., Effect of different mini-rib arrangements on endwall heat transfer in pin–fin channel, International Journal of Heat and Mass Transfer (2025). https://doi.org/10.1016/j.ijheatfluidflow.2024.109716.

[20] Ao et al., Effect of novel concentric annular fins on the melting and solidification process of stearic acid in thermal energy storage devices, Applied Thermal Engineering (2023). https://doi.org/10.1016/j.applthermaleng.2023.120855.

[21] Li et al., Effect of perforated fins on the heat-transfer performance of vertical shell-and-tube latent heat energy storage unit, Journal of Energy Storage (2021). https://doi.org/10.1016/j.est.2021.102647.

[22] Li et al., Effect of porous structure on the thermal and hydraulic features of combined heat sinks with open microchannels and pin-fins, International Journal of Heat and Mass Transfer (2025). https://doi.org/10.1016/j.ijthermalsci.2025.109933.

[23] Zhong et al., Effect of varying Reynolds numbers on the heat transfer and flow structure of vertical, curved, inclined, and serpentine pin fins, International Communications in Heat and Mass Transfer (2025). https://doi.org/10.1016/j.icheatmasstransfer.2024.108557.

[24] Wongcharoen et al., Effects of groove geometry around pin-fin perforation circumference on thermohydraulic behavior of pin-fin heat sinks under turbulent flow, Case Studies in Thermal Engineering (2025). https://doi.org/10.1016/j.csite.2025.106184.

[25] Yildirim et al., Enhancement of heat transfer by inclined holes through perforated heat sinks, International Journal of Heat and Mass Transfer (2025). https://doi.org/10.1016/j.ijthermalsci.2025.109810.

[26] Machi et al., Enhancing thermal efficiency of double-pass solar air collectors: A comparative study on the role of V-angled perforated fins, (Energy-) (2024). https://doi.org/10.1016/j.egyr.2024.06.048.

[27] Khelkar et al., Enhancing thermo-hydraulic performance of solar air heater system using hybrid pin-finned wavy absorber plate: numerical and experimental investigation, (Solar) (2026). https://doi.org/10.1016/j.solener.2026.114636.

[28] Ye et al., Evaluating the heat transfer characteristics of mesh-fed slot cooling configuration: Influence of slot height and pin-fin arrangement, Applied Thermal Engineering (2025). https://doi.org/10.1016/j.applthermaleng.2025.126304.

[29] Cui et al., Evaluation of a novel annular fin for heat transfer enhancement in hot water oil-displacement system, Thermal Science and Engineering Progress (2024). https://doi.org/10.1016/j.tsep.2024.102438.

[30] Ismail et al., Experimental and numerical analysis of heat sink using various patterns of cylindrical pin-fins, International Journal of Heat and Mass Transfer (2024). https://doi.org/10.1016/j.ijft.2024.100737.

[31] Liu et al., Experimental and numerical investigation of longitudinal and annular finned latent heat thermal energy storage unit, Solar Energy (2022). https://doi.org/10.1016/j.solener.2022.08.023.

[32] Hosseini et al., Experimental and numerical investigation of the melting behavior of a phase change material in a horizontal latent heat accumulator with longitudinal and annular fins, (Journal-o) (2024). https://doi.org/10.1016/j.est.2024.110563.

[33] Goveraiahgari et al., Experimental and numerical study on the influence of circular, oblong, teardrop and beetle pin fins on the enhancement of heat transfer in a wedge channel, (International-) (2025). https://doi.org/10.1016/j.ijthermalsci.2025.109751.

[34] Naik et al., Experimental investigation of melting and solidification characteristics in a vertical shell and tube latent heat thermal energy storage system with novel directional flow annular fins, (Journal-) (2025). https://doi.org/10.1016/j.est.2025.115768.

[35] Tiari et al., Experimental study of a latent heat thermal energy storage system assisted by varying annular fins, Journal of Energy Storage (2022). https://doi.org/10.1016/j.est.2022.105603.

[36] You et al., Experimental study of curvature effects on double-wall laminate cooling structure incorporating impingement hole, pin-fins and slot, Applied Thermal Engineering (2025). https://doi.org/10.1016/j.applthermaleng.2025.128427.

[37] doi:10.1016/j.expthermflusci.2006.01.001, Experimental Thermal and Fluid Science (2006). https://doi.org/10.1016/j.exptherm.

[38] Shin et al., Experimental study on natural convection from vertical cylinders with perforated plate fins, Applied Thermal Engineering (2024). https://doi.org/10.1016/j.applthermaleng.2024.123768.

[39] Li et al., Flow and heat transfer characteristics of droplet-shaped pin-fin channel under rotational conditions, International Journal of Heat and Mass Transfer (2025). https://doi.org/10.1016/j.ijheatmasstransfer.2025.127220.

[40] Hossain et al., Forced convective heat transfer over twisted and perforated forked pin fin heat sink: A numerical study, International Journal of Heat and Mass Transfer (2025). https://doi.org/10.1016/j.ijthermalsci.2025.109719.

[41] Danmaz et al., Geometric analysis of pin fin heat sinks: Effects of ellipticity and perforation for fin on heat transfer, Case Studies in Thermal Engineering (2025). https://doi.org/10.1016/j.csite.2025.106918.

[42] Mihalko et al., Harnessing transfer learning for achieving superior thermal-hydraulic performance in heterogeneous pin-fin arrays, International Communications in Heat and Mass Transfer (2025). https://doi.org/10.1016/j.icheatmasstransfer.2025.108968.

[43] Chowdhury et al., Heat transfer analysis in perforated pin fin heat sinks inspired by sterling gun barrel geometry, Case Studies in Thermal Engineering (2026). https://doi.org/10.1016/j.csite.2025.107524.

[44] Bilaskar et al., Heat transfer and acoustics investigation of a piezoelectric fan-porous finned heat sink system in the presence of channel flow, Thermal Science and Engineering Progress (2025). https://doi.org/10.1016/j.tsep.2025.103851.

[45] Sen et al., Heat transfer enhancement of air flow through new types of perforated dimple/protrusion fins, Applied Thermal Engineering (2024). https://doi.org/10.1016/j.applthermaleng.2024.124030.

[46] Demirkran et al., Hollowed and perforated fins in latent heat storage units for High-Temperature hybrid thermal energy storage applications, Energy Conversion and Management (2025). https://doi.org/10.1016/j.enconman.2025.119998.

[47] Alam et al., Investigating tetragonal prismatic pin-fins in microchannel heat sinks: Optimizing cooling performance, Thermal Science and Engineering Progress (2025). https://doi.org/10.1016/j.tsep.2025.103816.

[48] Ehsani et al., Investigating thermal performance enhancement in perforated pin fin arrays for cooling electronic systems through integrated CFD and deep learning analysis, Results in Engineering (2024). https://doi.org/10.1016/j.rineng.2024.102016.

[49] Li et al., Investigation on the thermal and hydraulic characteristics of the micro heat sinks with grooves and pin fins by Taguchi-based sensitivity analysis, (Applied-Th) (2024). https://doi.org/10.1016/j.applthermaleng.2024.123454.

[50] Kumar et al., Louvered finned car radiator with MWCNT-SiO2 hybrid nanofluid: An experimental approach, Powder Technology (2023). https://doi.org/10.1016/j.powtec.2022.118176.

[51] Jin et al., Multi-objective optimization of a microchannel pin-fin hybrid heat sink based on CFD and NSGA-II genetic algorithm, Case Studies in Thermal Engineering (2025). https://doi.org/10.1016/j.csite.2025.107467.

[52] Luo et al., Novel structural designs of fin-tube heat exchanger for PEMFC systems based on wavy-louvered fin and vortex generator by a 3D model in OpenFOAM, International Journal of (2021). https://doi.org/10.1016/j.ijhydene.2021.10.093.

[53] Chen et al., Numerical analysis of different finned tube designs in air heat exchangers for passive residual heat removal systems in LTHR, Nuclear Engineering and Design (2025). https://doi.org/10.1016/j.nucengdes.2025.114385.

[54] Gijoy et al., Numerical investigation and optimization of an asymmetric elliptical-cylindrical pin fin heat sink, International Journal of Heat and Mass Transfer (2025). https://doi.org/10.1016/j.ijthermalsci.2024.109514.

[55] Nawaz et al., Numerical investigation of forced convective heat transfer performance of slotted and twisted I-shaped pin fin heat sink, Case Studies in Thermal Engineering (2025). https://doi.org/10.1016/j.csite.2025.107352.

[56] Feleke et al., Numerical investigation of louver edges effect on the performances of louvered fin compact heat exchanger, Heliyon (2024). https://doi.org/10.1016/j.heliyon.2024.e27254.

[57] Wang et al., Numerical investigation on air-side heat transfer enhancement of wavy finned tube air cooler for underground tunnels, Applied Thermal Engineering (2025). https://doi.org/10.1016/j.applthermaleng.2025.126061.

[58] Rasangika et al., Numerical investigation on the thermal performance of perforated and non-perforated twisted fins at different twisting angles, Results in Engineering (2024). https://doi.org/10.1016/j.rineng.2024.102332.

[59] Han et al., Numerical investigations on the heat transfer characteristics of pin-fin heat sink for power converters in more electric aircraft, International Communications in Heat and Mass Transfer (2025). https://doi.org/10.1016/j.icheatmasstransfer.2025.108866.

[60] Agrawal et al., Numerical investigations on thermal performance of latent heat thermal energy storage system with novel corrugated annular fins in PCM, (Journal-of-) (2025). https://doi.org/10.1016/j.est.2025.116902.

[61] Ling et al., Numerical prediction of frosting growth characteristics of microchannel louvered fin heat exchanger, (Ener) (2023). https://doi.org/10.1016/j.energy.2023.128519.

[62] Zhu et al., Optimization of perforated plate-fin heat sink in electronic devices under radiation heat transfer, International Journal of Heat and Mass Transfer (2026). https://doi.org/10.1016/j.ijthermalsci.2025.110201.

[63] Kumar et al., Optimization of porous fin configurations in a solar receiver, Next Energy (2026). https://doi.org/10.1016/j.nxener.2026.100647.

[64] Alam et al., Optimization of tapered pin fins for enhanced heat transfer in microchannel heat sink, International Journal of Heat and Mass Transfer (2025). https://doi.org/10.1016/j.ijthermalsci.2025.109889.

[65] Tran et al., Optimization of the airside thermal performance of mini-channel-flat-tube radiators by using composite straight-and-louvered fins, International Journal of Heat and Mass Transfer (2020). https://doi.org/10.1016/j.ijheatmasstransfer.2020.120163.

[66] Han et al., Optimization of the annular fin arrangement in phase change heat storage units based on response surface methodology, Applied Thermal Engineering (2024). https://doi.org/10.1016/j.applthermaleng.2024.124479.

[67] Wang et al., Optimized design of vortex generator-like finned thermoelectric generator for waste heat energy harvesting, Applied Thermal Engineering (2025). https://doi.org/10.1016/j.applthermaleng.2025.127062.

[68] Machi et al., Optimizing double-pass solar air collector efficiency: Impact of a perforated discrete V-angled fins, Energy Reports (2025). https://doi.org/10.1016/j.egyr.2025.01.057.

[69] Prez et al., Parametric analysis of the influence of geometric variables of vortex generators on compact louver fin heat exchangers, Thermal Science and Engineering Progress (2022). https://doi.org/10.1016/j.tsep.2021.101151.

[70] Peng et al., Performance analysis of absorber tube in parabolic trough solar collector inserted with semi-annular and fin shape metal foam hybrid structure, (Case-Studies-) (2021). https://doi.org/10.1016/j.csite.2021.101112.

[71] Hu et al., Performance optimization of a wavy finned-tube heat exchanger with staggered curved vortex generators, International Journal of Heat and Mass Transfer (2023). https://doi.org/10.1016/j.ijthermalsci.2022.107830.

[72] Nie et al., Petal-shaped fin configurations for enhancing phase change material solidification in a horizontal shell and tube thermal energy storage unit, (Journal-of) (2025). https://doi.org/10.1016/j.est.2025.115685.

[73] Li et al., Polymer-based pin-fin microchannel heat exchangers: A comparative study of material and structural effects on performance, International Journal of Heat and Mass Transfer (2025). https://doi.org/10.1016/j.ijthermalsci.2024.109546.

[74] Tian et al., Proposing and thermo-economic optimization of an annular-thermoelectric gas heat recovery unit with a novel hybrid fin-pin vane and porous insert, (Applied-Th) (2023). https://doi.org/10.1016/j.applthermaleng.2023.121170.

[75] Fathi et al., Semi-porous-fin microchannel heat sinks for enhanced micro-electronics cooling, International Communications in Heat and Mass Transfer (2024). https://doi.org/10.1016/j.icheatmasstransfer.2024.107814.

[76] Zhang et al., Solidification of an annular finned tube ice storage unit, Applied Thermal Engineering (2022). https://doi.org/10.1016/j.applthermaleng.2022.118567.

[77] Zheng et al., Study on performance of carbon nanotube composite phase change cold storage sphere with annular fins, Journal of Energy Storage (2024). https://doi.org/10.1016/j.est.2023.110074.

[78] Yang et al., Taguchi optimization and thermoelectrical analysis of a pin fin annular thermoelectric generator for automotive waste heat recovery, (Renewab) (2024). https://doi.org/10.1016/j.renene.2023.119628.

[79] Dey et al., Temperature uniformity analysis of high concentrated photovoltaics (HCPV) arrangement using four quadrant pin fin and porous metal foam heatsink, Thermal Science and Engineering Progress (2025). https://doi.org/10.1016/j.tsep.2025.103818.

[80] Li et al., The influence of branched annular fins on the performance of phase change heat exchangers, International Journal of Heat and Mass Transfer (2025). https://doi.org/10.1016/j.ijheatfluidflow.2024.109714.

[81] Shahsavar et al., The numerical analysis in heat transfer, fluid flow, and irreversibility of a pin-fin heatsink under the ultrasonic vibration with different transducer power assignment scenarios, Thermal Science and Engineering Progress (2024). https://doi.org/10.1016/j.tsep.2024.102480.

[82] Zhang et al., The thermal management performance of the PCM-based pin fin heat sink under the transient heat flux shock conditions:An experimental study, International Communications in Heat and Mass Transfer (2025). https://doi.org/10.1016/j.icheatmasstransfer.2025.109809.

[83] Bakr et al., Thermal behavior and secondary flow analysis of perforated plate-fin heat sinks subjected to parallel and impinging flows, International Journal of Heat and Mass Transfer (2026). https://doi.org/10.1016/j.ijthermalsci.2026.110860.

[84] Ejaz et al., Thermal-hydraulic performance evaluation of airside of wavy fin compact heat exchangers under wet conditions, International Communications in Heat and Mass Transfer (2024). https://doi.org/10.1016/j.icheatmasstransfer.2024.107685.

[85] Yang et al., Thermal-hydraulic performance of super-amphiphobic louver-fin flat-tube heat exchanger under fouled condition, Applied Thermal Engineering (2023). https://doi.org/10.1016/j.applthermaleng.2023.121142.

[86] Lin et al., Thermal-hydraulic performance optimization of louver-finned round tube heat exchangers with rear-punched curved delta-winglet generators using Taguchi and response surface methods, International Journal of Thermal Sciences (2026). https://doi.org/10.1016/j.ijthermalsci.2026.110910.

[87] Chand et al., Thermal performance enhancement of solar air heater using louvered fins collector, Solar Energy (2022). https://doi.org/10.1016/j.solener.2022.04.046.

[88] Alshibil et al., Thermodynamical analysis and evaluation of louver-fins based hybrid bi-fluid photovoltaic/thermal collector systems, Renewable Energy (2023). https://doi.org/10.1016/j.renene.2023.02.105.

[89] Yang et al., Topological optimization design of micro-pin fin heat sinks for high heat flux cooling application, International Journal of Heat and Mass Transfer (2025). https://doi.org/10.1016/j.ijthermalsci.2025.110102.